PERK Regulates Epithelial–Mesenchymal Transition Through Autophagy and Lipid Metabolism in Lens Epithelial Cells

Xiaoran Wang, Baoxin Chen, Jieping Chen, Mi Huang, and Shan Huang

State Key Laboratory of Ophthalmology, Zhongshan Ophthalmic Center, Sun Yat-Sen University, Guangdong Provincial Key Laboratory of Ophthalmology Visual Science, Guangzhou, China

Correspondence: Shan Huang, Zhongshan Ophthalmic Centre, Sun Yat-Sen University, 54 Xianlie Rd., Guangzhou 510060, China; huangsh29@mail.sysu.edu.cn.

Received: January 21, 2025
Accepted: April 21, 2025
Published: May 23, 2025

Citation: Wang X, Chen B, Chen J, Huang M, Huang S. PERK regulates epithelial–mesenchymal transition through autophagy and lipid metabolism in lens epithelial cells. *Invest Ophthalmol Vis Sci.* 2025;66(5):35. https://doi.org/10.1167/iovs.66.5.35

Purpose. Pathological epithelial–mesenchymal transition (EMT) of lens epithelial cells (LECs) plays a crucial role in the formation of lens fibrosis, particularly in fibrotic posterior capsular opacification and anterior subcapsular cataract (ASC). Here we investigated the potential roles of endoplasmic reticulum (ER) stress in the development of lens fibrosis.

Methods. RNA sequencing was performed to examine global gene expression changes in patients with ASC, as well as in TGFβ2-induced human lens explants and rabbit primary LECs. Rabbit LECs were treated with TGFβ2 in the presence or absence of the ER stress modulator, PERK inhibitor ISRIB, and autophagy inducer for in vitro studies. In vivo investigations were carried out using a mouse model of injury-induced capsular fibrosis, with ISRIB administration. To uncover the underlying mechanisms, we conducted lipidomics analysis, transmission electron microscopy, immunostaining, quantitative PCR, Western blot, and capillary Western immunoassay.

Results. ER stress genes were upregulated in patients with ASC, TGFβ2-stimulated human explants and primary LECs. Pharmacologic ER stress induction promoted EMT, while its inhibition reduced TGFβ2-induced mesenchymal gene levels. Blocking the PERK axis of ER stress with ISRIB or targeting downstream factor ATF4 suppressed EMT, whereas the IRE1 axis showed no effect. Consistent with these in vitro observations, anterior chamber injection of ISRIB also reduced subcapsular plaque formation in a mouse model of lens fibrosis by suppressing SMAD2/3 activation. Mechanistically, ISRIB suppressed LC3-II conversion and P62 degradation, indicating autophagy suppression. Lipidomics revealed phosphatidylethanolamine (PE), essential for autophagosome formation, was downregulated in TGFβ2-treated LECs and upregulated with ISRIB cotreatment. Inducing autophagy with rapamycin significantly rescued the mesenchymal gene suppression by ISRIB, whereas autophagy inhibitor CQ produced opposite effects.

Conclusions. ER stress, particularly the PERK axis, promotes LECs' EMT through autophagy and PE metabolism, offering potential therapeutic targets for the treatment of lens fibrosis.

Keywords: epithelial–mesenchymal transition, PERK, autophagy, cataract

Cataracts are the most common vision-threatening disease worldwide. Surgical intervention is the only effective therapy. However, a significant proportion of postoperative patients develop posterior capsular opacification (PCO), which leads to secondary vision impairment.[1] PCO and anterior subcapsular cataract (ASC) share a common pathological mechanism, primarily the abnormal epithelial–mesenchymal transition (EMT) of lens epithelial cells (LECs), leading to subcapsular fibrotic opacification, particularly following a penetrating injury or cataract surgery.[2] Notably, PCO occurs in most pediatric patients after lens removal if prophylactic posterior capsulotomy is not performed and can significantly impair visual function, emphasizing the urgent need to develop new treatment strategies.[3,4] EMT, which involves the transformation of LECs into spindle-shaped mesenchymal cells, is considered the key pathogenesis underlying lens fibrosis.[3,5,6] Lens fibrosis is characterized by the excessive accumulation of extracellular matrix (ECM) proteins in response to cytokines present in the aqueous humor, primarily transforming growth factor β2 (TGFβ2) induced by cataract surgery or injury. This process progressively remodels the tissue architecture and ultimately contributes to the formation of fibrotic plaques beneath the lens capsule.[7] Thus, understanding the exact mechanisms of pathological EMT in the lens is crucial for identifying the underlying cause and possible therapeutic targets of lens fibrosis.

The endoplasmic reticulum (ER) is the primary organelle for the folding and modification of nascent transmembrane and secreted proteins, as well as the site of synthesis for important lipids. Although this process is tightly regulated, various external factors can disrupt ER proteostasis, lead-

ing to a state of ER stress and ER expansion caused by the accumulation of misfolded and unfolded proteins. To restore ER homeostasis, three ER stress sensors (IRE1α, PERK, and ATF6) activate a set of signal transduction cascades, collectively termed the unfolded protein response (UPR).[8] There is evidence indicating that the ER stress is activated in many fibrotic diseases.[9–11] However, the role of ER stress in lens fibrosis and its underlying mechanism remains unclear.

During lens fibrosis, transdifferentiated lens epithelial cells are highly secretory, which results in high protein-folding demand. Therefore, we investigated the function of ER stress in the development of lens fibrosis. This study demonstrated that ER stress is triggered during ASC and TGFβ2-induced EMT in LECs, which in turn enhances the EMT process. Pharmacological targeting of the PERK/ATF4 branch of the ER stress with ISRIB largely prevented the EMT process in LECs and injury-induced lens fibrosis in mice. Mechanistically, autophagy was activated to potentiate the EMT of LECs upon TGFβ2 stimulation, which could be inhibited by ISRIB both in vitro and in vivo. Overall, we demonstrated the indispensable role of the PERK/ATF4 stress response pathway in supporting the mesenchymal transition of the lens epithelium, which may serve as an attractive therapeutic strategy to combat lens fibrosis and other fibrotic disorders.

Materials and Methods

Animal Experiments

All experiments were performed in accordance with the Declaration of Helsinki and the ARVO Statement for the Use of Animals in Ophthalmic and Vision Research. All investigations were approved by the Institutional Animal Care and Use Committee of Zhongshan Ophthalmic Center. 6- to 8-week-old C57BL/6 mice were used for the injury-induced capsular fibrosis model as described previously.[12] Tropicamide eye drops dilated the pupil, whereas proparacaine hydrochloride eye drops provided anesthesia. A 26-gauge hypodermic needle was inserted vertically through the cornea to make a small incision at the center of the anterior capsule, reaching a depth of approximately 300 µm in the right eye. For drug treatment, 2 µL ISRIB (5 µM, S0706; Selleckchem, Houston, TX, USA) was injected into the anterior chamber of the injured eye with a 30-gauge Hamilton microsyringe. The same volumes of PBS were injected into the control group.

Cell Culture and Treatment

Rabbit primary lens epithelial cells were prepared as previously described.[13] In brief, lens capsules from 2-month-old New Zealand white rabbits were cut into 1 × 1-mm^2 pieces and cultivated in minimum essential media supplemented (11095080; Thermo Fisher Scientific, Waltham, MA, USA) with 10% fetal bovine serum (10099141C; Gibco, Grand Island, NY, USA), NEAA (11140050; Thermo Fisher Scientific), and antibiotics (15140122; Thermo Fisher Scientific). TGFβ2 (5 ng/mL; 302-B2-010; R&D Systems, Minneapolis, MN, USA), 4µ8C (S7272; Selleckchem), or ISRIB was added to the culture medium. LECs from passages 3 to 5 were utilized for subsequent cell experiments.

Transfection With Small Interfering RNA

To silence ATF4 expression, rabbit primary lens epithelial cells were transfected with ATF4-specific small interfering RNAs (siRNAs) along with nontargeting siRNAs (Qingke, Beijing, China) as a negative control. Transfection was carried out using Lipofectamine 3000 (l3000015; Thermo Fisher Scientific) reagent for 48 hours. The Alexa Fluor Red positive control was used to assess the transfection efficiency, with all siRNAs applied at a concentration of 50 nM. The efficacy of siRNA transfection was validated via real-time PCR. Supplementary Table S1 contains the siRNA sequences used.

Whole-Mount Staining and Immunofluorescence

The whole-mount lens anterior capsules were dissected along the lens equator region and flattened on glass slides. Tissues or cells were fixed with 4% paraformaldehyde for 20 minutes at room temperature and blocked in 0.3% Triton X-100/PBS solution containing 3% bovine serum albumin for 30 minutes, followed by an overnight incubation with primary antibodies (1:100) at 4°C. After incubation with fluorochrome-conjugated secondary antibodies (1:1000), the tissues or cells were thoroughly rinsed and counterstained with DAPI. Fluorescent signals were captured via a fluorescence microscope (Leica, DM4000, Wetzlar, Germany) or a confocal fluorescence microscope (Zeiss, LSM800, Oberkochen, Germany). The primary antibodies (1:100) used for immunofluorescence were as follows: Smad2/3 (8685; Cell Signaling Technology, CST, Danvers, MA, USA), p-Smad2/3 (AF3367; Affinity Biosciences, Cincinnati, OH, USA), α-SMA (ab7817; Abcam, Cambridge, UK), FN (ab2413; Abcam), BiP (3177; CST), and P62 (ab56416; Abcam).

Transmission Electron Microscopy

After the indicated treatment, the LECs were fixed with 2.5% glutaraldehyde in 0.1 M cacodylate buffer (pH 7.4) at 4°C overnight and postfixed in 1% osmium (VIII) oxide (OsO_4) and uranyl acetate. The samples were then dehydrated in ethanol and embedded in epoxy resin. Ultrathin slices of 60 to 90 nm in size were stained with a uranium acetate–saturated alcohol solution and lead citrate and examined under a Hitachi (HT7700, Tokyo, Japan) transmission electron microscope system.

Lens Collection and RNA Sequencing

Human ASC lenses and normal lenses were collected from organ donors provided by the Eye Bank of Zhongshan Ophthalmic Center in accordance with the Declaration of Helsinki. Human lens explants from healthy individuals or primary cultured LECs were isolated and cultured in DMSO or 5 ng/mL TGFβ2 for 48 hours. As a single lens capsule was not sufficient for RNA sequencing (RNA-seq), three samples were pooled for RNA isolation. Sequencing was conducted via the NEBNext Ultra RNA Library Prep Kit for Illumina (New England Biolabs (NEB), Ipswich, MA, USA), and the samples were sequenced on the Illumina HiSeq platform. All sequencing data used in this study have been deposited (PRJCA037110) in the Genome Sequence Archive (Genomics, Proteomics & Bioinformatics 2021)[14] in the National Genomics Data Center (Nucleic Acids Res 2022),[15] China National Center for Bioinforma-

Investigative Ophthalmology & Visual Science

tion/Beijing Institute of Genomics, Chinese Academy of Sciences, under the Accession codes HRA010734 for ASC and normal lenses, HRA010750 for human lens epithelial explants, and CRA023843 for rabbit primary LECs, and they are accessible upon request at https://ngdc.cncb.ac.cn. The sequencing results were mapped to the human reference genome via HISAT2. Differentially expressed genes were determined at $P < 0.05$ and log2|FC| >1. Gene Ontology (GO) analysis was performed with R statistical software. RNA sequencing data and associated information for GSE206574[16] were obtained from the GEO database to investigate gene expression changes following cataract surgery in a mouse lens fiber cell removal model.

Lipidomics Analysis

Sample preparation involved extracting cell samples with MTBE/MeOH (3:1, v/v) containing internal standards, followed by centrifugation and reconstitution in mobile phase B for liquid chromatography/tandem mass spectrometry (MS) analysis. Lipid profiling was performed on a UPLC system (Accucore C30 column, Thermo Fisher Scientific) with a gradient solvent system and an electrospray ionization quadrupole linear ion trap tandem mass spectrometer (ESI-QTRAP-MS/MS) system operating in positive and negative ion modes. The system parameters included a 45°C column temperature, a 0.35-mL/min flow rate, and specific multiple reaction monitoring (MRM) transitions optimized for metabolite detection. Data analysis included principal component analysis (PCA) using the prcomp function in R, hierarchical clustering and Pearson correlation analysis with the ComplexHeatmap package, and differential metabolite selection via partial least squares-discriminant analysis (PLS-DA) (variable importance in projection (VIP) ≥ 1, $|\text{Log2FC}| \geq 1$). Kyoto Encyclopedia of Genes and Genomes (KEGG) annotation and pathway enrichment were performed to map metabolites to pathways and identify significant enrichments with a hypergeometric test.

Western Blot Analysis

The cells were lysed with RIPA buffer (P0013C; Beyotime, Shanghai, China) with a protease inhibitor cocktail (04906837001; Roche, Basel, Switzerland) and quantified with a BCA assay (P0012; Beyotime). The samples were electrophoresed on SDS-PAGE gels and then transferred to a PVDF membrane. The membranes were blocked in TBST solution containing 5% nonfat milk, followed by an overnight incubation with primary antibodies (1:1000) at 4°C. The membranes were subsequently incubated with secondary antibodies (1:2000) for 2 hours at room temperature. The immunodetection was visualized with an ECL substrate via a Bio-Rad (Hercules, CA, USA) detection system. The primary antibodies (1:1000) used in Western blot analysis were as follows: GAPDH (2118; CST), BiP (3177; CST), ACTIN (3700; CST), p-eIF2α (9721; CST), eIF2α (9722; CST), IRE1α (3294; CST), vimentin (5741; CST), β-catenin (8480; CST), LC3 (12741; CST), p-SMAD2/3 (8828; CST), SMAD2/3 (8685; CST), FN (ab137720; Abcam), α-SMA (ab7817; Abcam), and P62 (ab56416; Abcam).

Capillary Western Immunoassay (Wes)

Lens capsules were lysed with RIPA buffer with protease inhibitor cocktail (Thermo Fisher Scientific) and quantified with a BCA assay (Beyotime). Wes analysis was performed on a Wes system (ProteinSimple; Bio-Techne, Minneapolis, MN, USA) according to the manufacturer's instructions via a Wes separation kit and an anti-rabbit detection module for Wes. The antibodies used were the same as those used for Western blotting.

RNA Isolation and Quantitative RT-PCR

The RNA was purified via an RNA isolation kit (74104; Qiagen, Hilden, Germany) and quantified via a NanoDrop spectrophotometer (Thermo Fisher Scientific). cDNAs were synthesized with PrimeScript RT Master Mix (RR036A; Takara Bio, Inc., Kutsatsu, Japan). Quantitative PCR (qPCR) was performed via the use of ChamQ SYBR Color qPCR Master Mix (Q431-02; Vazyme, Nanjing, China) on a StepOnePlus real-time PCR system (Applied Biosystems, Waltham, MA, USA) according to the manufacturer's protocol. The expression levels were normalized to those of ACTIN or GAPDH. The sequences of the primers (5′−3′) used are listed in Supplementary Table S1.

Statistics

All the data are expressed as the means ± SDs. Statistical analyses were performed via GraphPad (GraphPad Software, La Jolla, CA, USA). Student's *t*-test was used to compare differences between groups. One-way ANOVA was used to compare differences among three or more groups. $P < 0.05$ was considered statistically significant.

Results

Molecular Characteristics of Lens Fibrosis and TGFβ2-Stimulated LECs

We first conducted RNA-seq on lens capsules from healthy individuals and patients with ASC to explore the molecular characteristics of lens fibrosis. Our findings highlight a prominent increase in the expression of EMT-related genes and the activation of extracellular matrix structural constituents and growth factor binding in samples from patients with ASC (Fig. 1A). TGFβ2 is recognized as a key initiator of lens fibrosis. Therefore, we performed RNA-seq on human lens explants (Fig. 1B) and primary cultured rabbit LECs (Fig. 1C) after exposure to TGFβ2. Importantly, the most significantly altered pathways closely resembled those observed in patient samples. The exposure of LECs to TGFβ2 led to increased expression of the mesenchymal markers FN and α-SMA, along with a shift to a prolonged mesenchymal morphology (Fig. 1D). We also established a mouse model of injury-induced capsular fibrosis to mimic lens fibrosis after a penetrating injury or after cataract surgery and observed α-SMA expression and fibronectin production in lens epithelial cells (Fig. 1E). The injury-induced capsular fibrosis mouse model, along with TGFβ2-stimulated LECs, was adopted for further exploration of the mechanism and therapeutic targets for lens fibrosis.

ER Stress Is Activated During the EMT Process of LECs

We noted that pathway analysis revealed increased expression of endoplasmic reticulum (ER) lumen genes (Fig. 2A), along with a significant increase in ER stress gene expression in ASC patient samples. To explore whether ER stress was induced during the EMT process in lens fibrosis, we

Investigative Ophthalmology & Visual Science

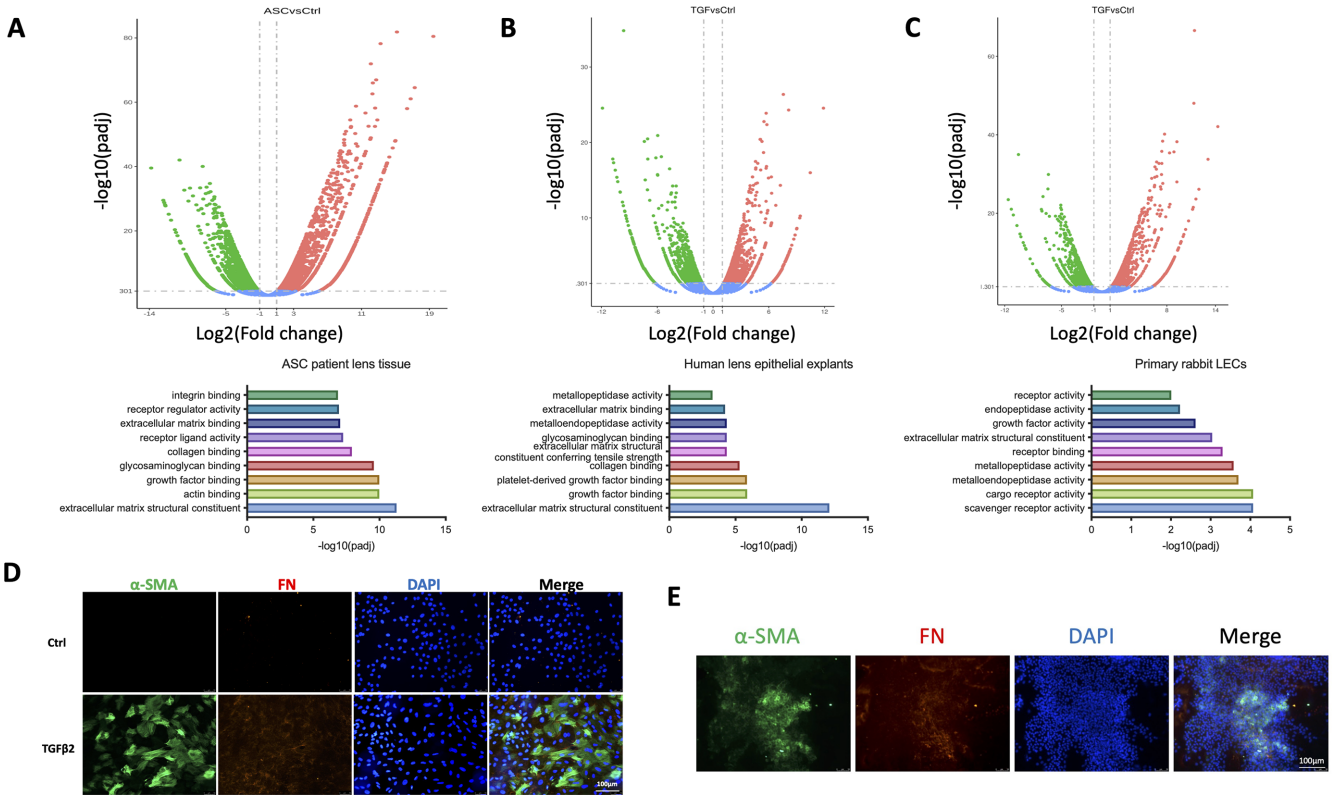

Figure 1. Molecular characteristics of lens fibrosis and TGFβ2-stimulated LECs. Volcano plots of differential gene expression and enriched pathway analysis were conducted in lens capsules from healthy individuals and patients with ASC (**A**), human lens explants (**B**), and primary cultured rabbit lens epithelial cells (**C**) treated with 5 ng/mL TGFβ2 for 48 hours. (**D**) Immunofluorescence staining of α-SMA and FN in LECs treated with or without TGFβ2 (5 ng/mL) for 48 hours. (**E**) Immunofluorescence staining of α-SMA and FN in subcapsular plaques of the fibrotic mouse model. *Scale bar*: 100 µm.

tested the expression of BiP, a critical ER stress marker, in the capsular fibrosis mouse model. Both the immunostaining and Wes results revealed increased expression of BiP in the capsular fibrosis group (Figs. 2B, 2C). Consistent with the in vivo findings, TGFβ2 treatment upregulated the expression of BiP (Fig. 2D) and activated key ER stress sensors at both the mRNA and protein levels in LECs (Figs. 2E, 2F), indicating that TGFβ2 induced ER stress in a time- and dose-dependent manner. LECs exhibited ER expansion upon exposure to TGFβ2, which is consistent with the increased secretory output during EMT (Fig. 2G). Taken together, these data indicate that ER stress is induced in the capsular fibrosis mouse model and TGFβ2-induced EMT.

Reciprocal Regulation Between ER Stress and EMT in LECs

In the acute response of LECs to lens fiber cell removal, which models cataract surgery in mice, there is a rapid upregulation of ER stress genes (Fig. 3A). At this time point, fibrotic markers such as *Fn* and *α-Sma*, which are commonly associated with lens fibrosis, are not significantly upregulated in LECs.[16] We then investigated whether ER stress contributes to the progression of EMT as a potential mechanism for fibrotic remodeling. LECs were exposed to the SERCA pump inhibitor thapsigargin (TG) for 40 hours, resulting in an increase in BiP protein levels, indicating ER stress activation (Fig. 3B). Importantly, TG dose-dependently upregulated the expression of mesenchymal genes, such as α-SMA, β-catenin, and FN in LECs (Fig. 3B). We also found that a high dose of TG (1 µM) even increased EMT gene expression within 6 hours while downregulating the epithelial gene E-cadherin in LECs (Fig. 3C). Additionally, treatment with tunicamycin, another established ER stress inducer, also led to the upregulation of EMT genes (Fig. 3D). Moreover, 4-PBA, a chemical chaperone that attenuates ER stress, prevented TGFβ2-stimulated fibronectin upregulation (Fig. 3E). Together, these findings suggest that ER stress may contribute to the EMT process and that pharmacologic inhibition of ER stress might impede EMT progression.

PERK/ATF4 Is Required for TGFβ2-Induced EMT but Not the IRE1/XBP1 Branch

The PERK and IRE1α branches, central to ER stress, play unique roles in transmitting regulatory signals under stress conditions. We observed that the expression of both ATF4 and XBP1, downstream targets of the PERK and IRE1α pathways, continually increased upon TGFβ2 treatment (Fig. 4A). We thus wondered whether the activation of these pathways contributes critically to the mesenchymal transition of LECs. To this end, ISRIB (a PERK/p-eIF2α inhibitor) and 4µ8C (an IRE1α inhibitor) were used to pharmacologically inhibit the PERK/ATF4 and IRE1/XBP1 branches of the ER stress, respectively. Notably, ISRIB treatment abolished the activation of FN and α-SMA mediated by TGFβ2 at the mRNA and protein levels (Figs. 4B–D). However, inhibiting the IRE1/XBP1 pathway using 4µ8C had no impact on

Investigative Ophthalmology & Visual Science

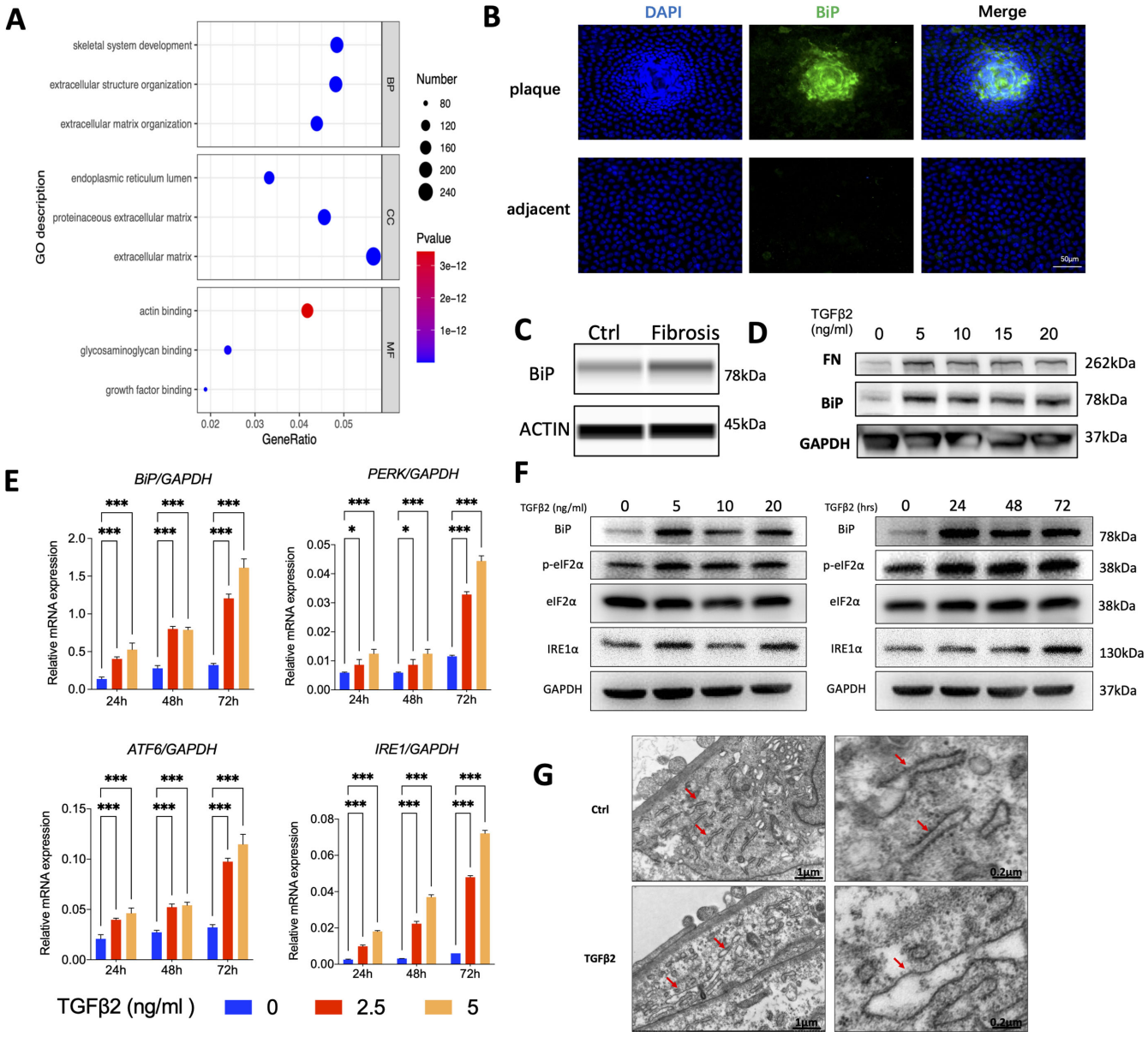

Figure 2. ER stress is activated during the EMT process of LECs. (**A**) Gene Ontology analysis of differentially expressed genes (DEGs) in patients with ASC was performed, and the top enriched pathways are shown. (**B**) The expression of the ER stress marker BiP in capsular fibrosis mice was evaluated by immunofluorescence staining. *Scale bar*: 50 μm. (**C**) Capillary Western immunoassay was used to evaluate BiP expression in capsular fibrosis mice. (**D**) The expression of FN and BiP in LECs treated with increasing doses of TGFβ2 was detected by Western blotting. (**E**) The expression of ER stress sensors in LECs treated with increasing durations or doses of TGFβ2 was detected by quantitative RT-PCR. (**F**) Western blotting was used to detect the expression of ER stress sensors in LECs treated with increasing durations or doses of TGFβ2. (**G**) The ER was visualized via transmission electron microscopy, where red arrows mark the ER. $^{*}P < 0.05$, $^{***}P < 0.001$ versus the control group.

profibrotic gene expression. Similarly, other IRE1α RNase and kinase inhibitors did not alter FN expression (Supplementary Fig. S1). The dose-dependent inhibitory effect of ISRIB on α-SMA was also shown by western blot analysis (WB) (Fig. 4E). Given that ATF4 is the pivotal effector of the PERK pathway, we genetically blocked ATF4 function with siRNA to further investigate its role in EMT (Fig. 4F). Consistently, genetic targeting of ATF4 also prevented the upregulation of the mesenchymal markers FN and α-SMA (Figs. 4F, 4G). Collectively, these results suggest that the PERK/ATF4 branch of the UPR, but not the IRE1/XBP1 branch, is specifically required for the EMT process in LECs.

ISRIB Suppresses Fibrotic Plaque Formation In Vivo

On the basis of the in vitro results, we next investigated whether ISRIB could also suppress lens fibrosis in vivo. LECs are stimulated to undergo hyperproliferation and EMT by puncturing the anterior capsule through needle injury (Fig. 5A). Obvious opacities beneath the lens capsule were observed in the control group, whereas the ISRIB-treated group developed limited capsular opacities (Fig. 5B). We also evaluated the molecular changes after injury through immunofluorescence staining of whole-mount lens anterior

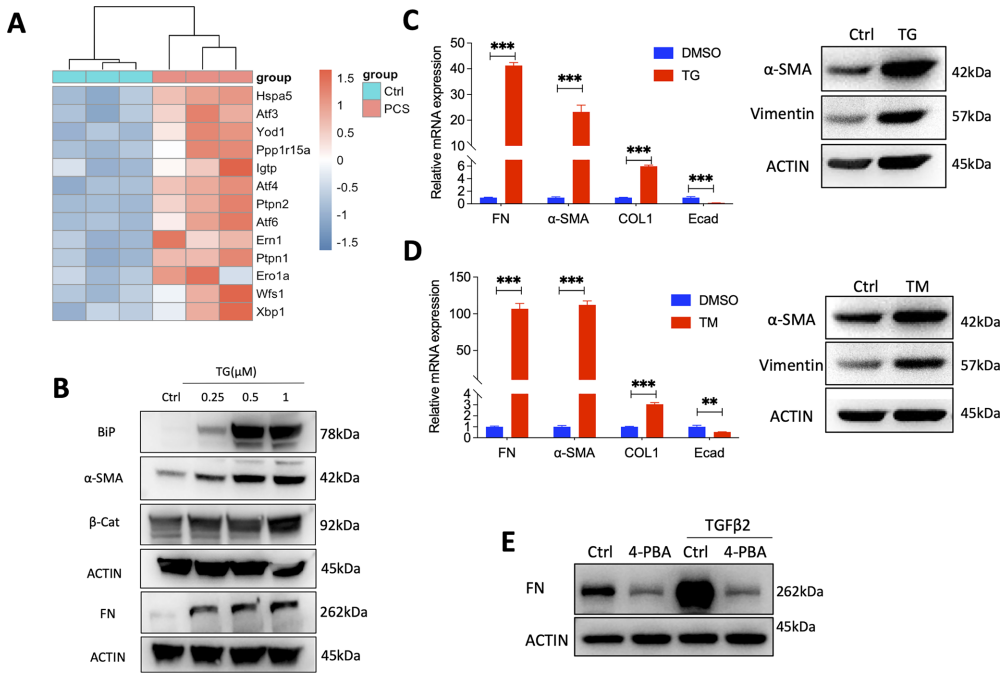

Figure 3. Reciprocal regulation between ER stress and EMT in LECs. (**A**) Heatmap analysis of the ER stress signature in LECs at 0 and 6 hours postcataract surgery (PCS). (**B**) The expression of BiP, α-SMA, β-catenin, and FN in LECs treated with increasing doses of TG for 40 hours was detected by Western blotting. EMT gene expression in LECs treated with thapsigargin (1 μM) (**C**) or tunicamycin (5 μg/mL) (**D**) for 6 hours. (**E**) The effect of 4-PBA on the expression of FN in LECs was evaluated by Western blotting. $^{**}P < 0.01$, $^{***}P < 0.001$ versus the control group.

capsules. As shown in Figure 5C, while puncture stimulated α-SMA expression, the ISRIB-treated mice presented less α-SMA accumulation, which is consistent with the slit-lamp images.

ISRIB Partially Blocks SMAD2/3 Activation

It is well established that the canonical TGFβ2/SMAD2/3 signaling pathway plays a crucial role in fibrotic disorders, including EMT in LECs.[17,18] To investigate whether ISRIB regulates EMT through this pathway, we examined SMAD2/3 phosphorylation and nuclear translocation both in vitro and in vivo. As expected, TGFβ2 stimulation significantly increased SMAD2/3 phosphorylation and promoted its nuclear translocation in LECs, confirming activation of the SMAD2/3 signaling cascade. However, ISRIB treatment attenuated SMAD2/3 phosphorylation and reduced its nuclear localization, indicating partially inhibition of SMAD2/3 activation (Figs. 6A, 6B). Consistent with these findings, in vivo immunofluorescence analysis revealed that SMAD2/3 was predominantly localized in the cytoplasm but also translocated into the nucleus in the control group, suggesting active SMAD signaling. In contrast, in ISRIB-treated mice, SMAD2/3 was largely retained in the cytoplasm with reduced nuclear accumulation, further supporting that ISRIB suppresses SMAD2/3 signaling activation in vivo (Figs. 6C, 6D).

ISRIB Regulate Phosphatidylethanolamine Metabolism in LECs

Since the ER is a primary site for the synthesis of various lipids, we conducted a comprehensive lipidomics analysis in control, TGFβ2-treated, and TGFβ2 + ISRIB-cotreated LECs to evaluate the effect of ISRIB on lipid metabolism. A total of four differential lipid classes and 130 differential lipid metabolites were identified between the TGFβ2 and control groups. Of these, 100 lipid metabolites were downregulated, with the majority belonging to glycerophospholipids (Fig. 7A). Additionally, k-means clustering analysis was performed to investigate the dynamic changes in lipid profiles across the three groups (Fig. 7B). All identified lipids were grouped into nine clusters based on their standardized relative abundance in each condition. Notably, clusters 4 and 5 exhibited a decrease following TGFβ2 treatment, with a subsequent increase upon cotreatment with TGFβ2 and ISRIB. PE(P-20:0_20:3) was one of the most significantly altered metabolites (Figs. 7C, 7D). Additionally, the autophagy pathway was the most enriched cellular process in KEGG analysis, with only phosphatidylethanolamine (PE) species being significantly represented. PE species were downregulated in the TGFβ2 group and upregulated in the TGFβ2 + ISRIB cotreatment group (Fig. 7E). PE is synthesized in the endoplasmic reticulum through the CDP-ethanolamine pathway and, with the assistance of ATG3 and ATG7, conjugates to LC3-I to form LC3-I–PE (LC3-II). This complex is then recruited to the membranes of autophagosomes, playing a crucial role in autophagy.

ISRIB Attenuates TGFβ2-Mediated Autophagy

Our previous research also demonstrated that autophagy was activated to potentiate the EMT of LECs upon TGFβ2 stimulation.[19] It has also been reported that ER stress can induce adaptive autophagy.[20,21] Therefore, we investigated whether the PERK/ATF4 branch of the ER stress

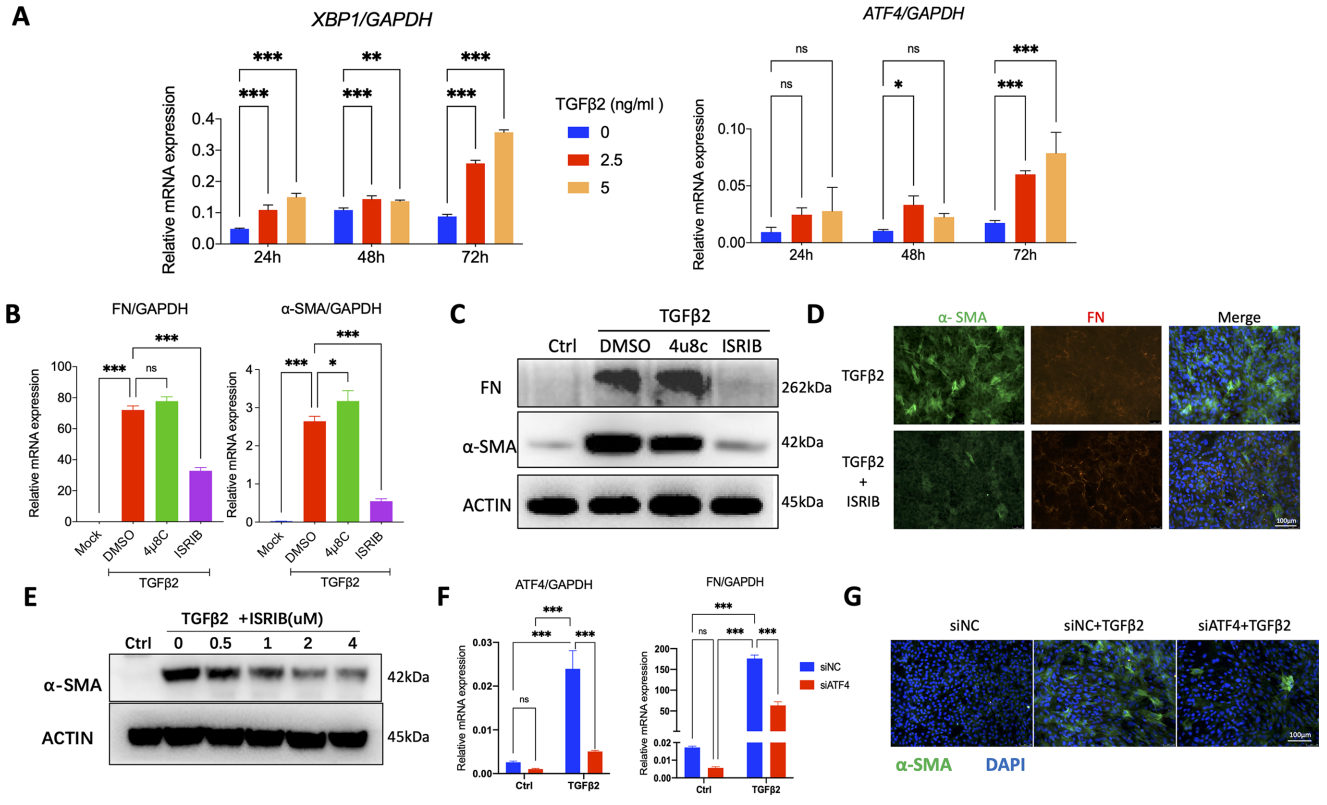

Figure 4. PERK/ATF4, but not the IRE1/XBP1 branch, is required for TGFβ2-induced EMT. (**A**) XBP1 and ATF4 expression in LECs treated with increasing durations or doses of TGFβ2 was detected by quantitative RT-PCR. (**B, C**) The expression of EMT-related molecules in LECs incubated with TGFβ2 and 4μ8C (25 μM) or ISRIB (4 μM) for 72 hours was detected via quantitative RT-PCR and western blot analysis (WB). (**D**) Immunofluorescence staining of α-SMA and FN in LECs treated with or without TGFβ2 and ISRIB for 72 hours. (**E**) α-SMA levels in LECs treated with TGFβ2 and increasing doses of ISRIB were detected by WB. (**F, G**) ATF4 knockdown efficiency and the effects of ATF4 knockdown on FN and α-SMA expression were measured via quantitative RT-PCR and immunofluorescence staining. *Scale bar*: 100 μm. *P < 0.05, **P < 0.01, ***P < 0.001 versus the control group.

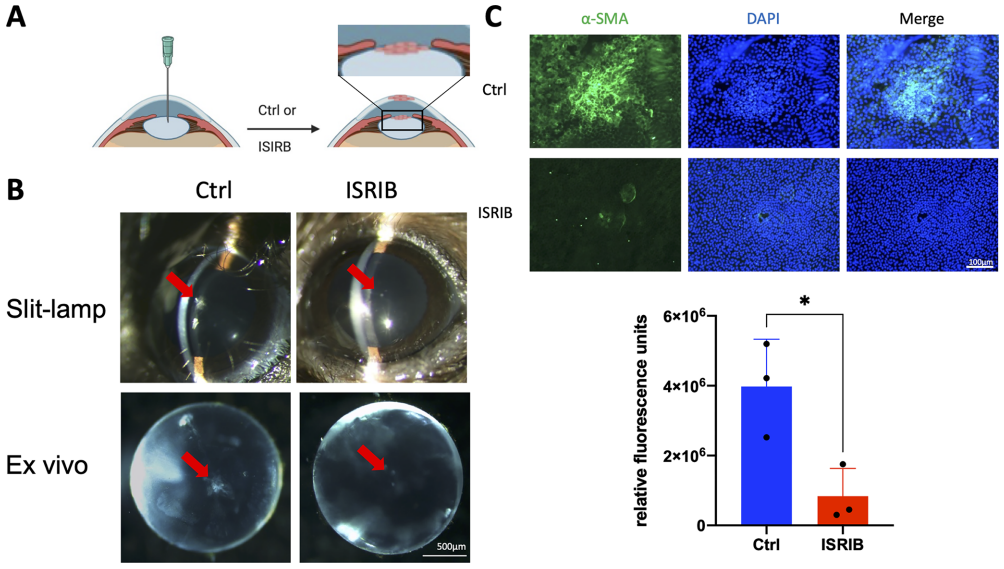

Figure 5. ISRIB suppresses fibrotic plaque formation in vivo. (**A**) Schematic diagram of the mouse model of injury-induced capsular fibrosis. (**B**) Representative slit-lamp microscope and ex vivo images of control and ISRIB-treated mice 7 days after injury. The formation of irregular fibrotic opacity is indicated by *red arrows*. *Scale bar*: 500 μm. (**C**) Immunofluorescence staining of lens capsule whole mounts from control and ISRIB-treated mice and quantification of the α-SMA signal. *Scale bar*: 100 μm. *P < 0.05.

Investigative Ophthalmology & Visual Science

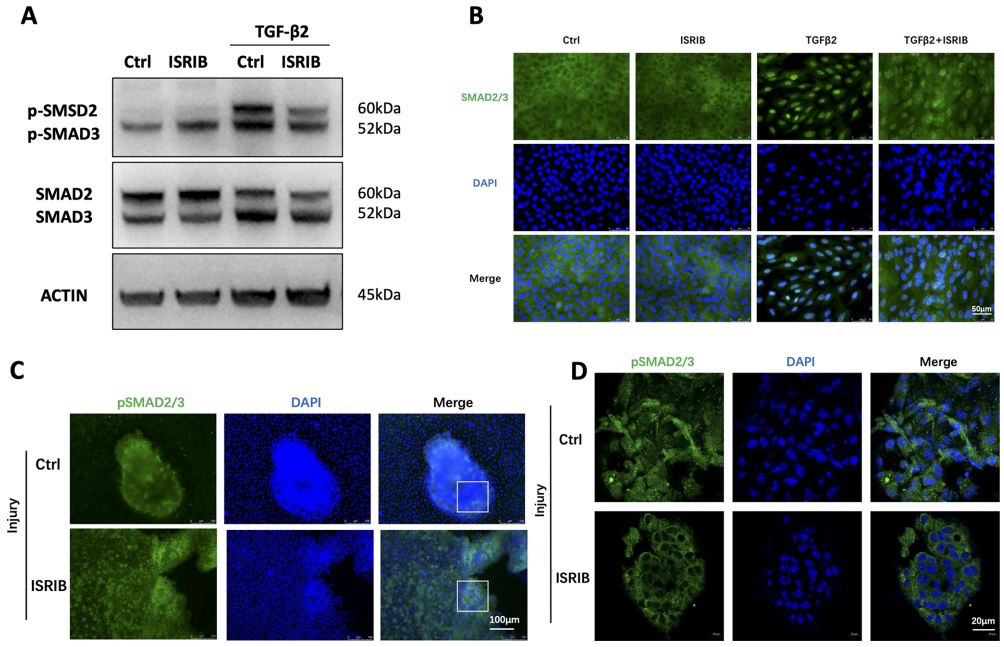

Figure 6. ISRIB partially blocks SMAD2/3 activation. (**A**) Western blot analysis of p-SMAD2, p-SMAD3, and total SMAD2/3 levels in LECs incubated with TGFβ2 and ISRIB. (**B**) Immunofluorescence staining of SMAD2/3 in LECs treated with or without TGFβ2 and ISRIB for 48 hours. *Scale bar*: 50 μm. (**C**) Immunofluorescence staining of lens capsule whole mounts from control and ISRIB-treated mice showing p-SMAD2/3 signals. The *boxed area* indicates the magnified region. *Scale bar*: 100 μm. (**D**) The intracellular localization of p-SMAD2/3 in plaques was confirmed by confocal microscopy. *Scale bar*: 20 μm.

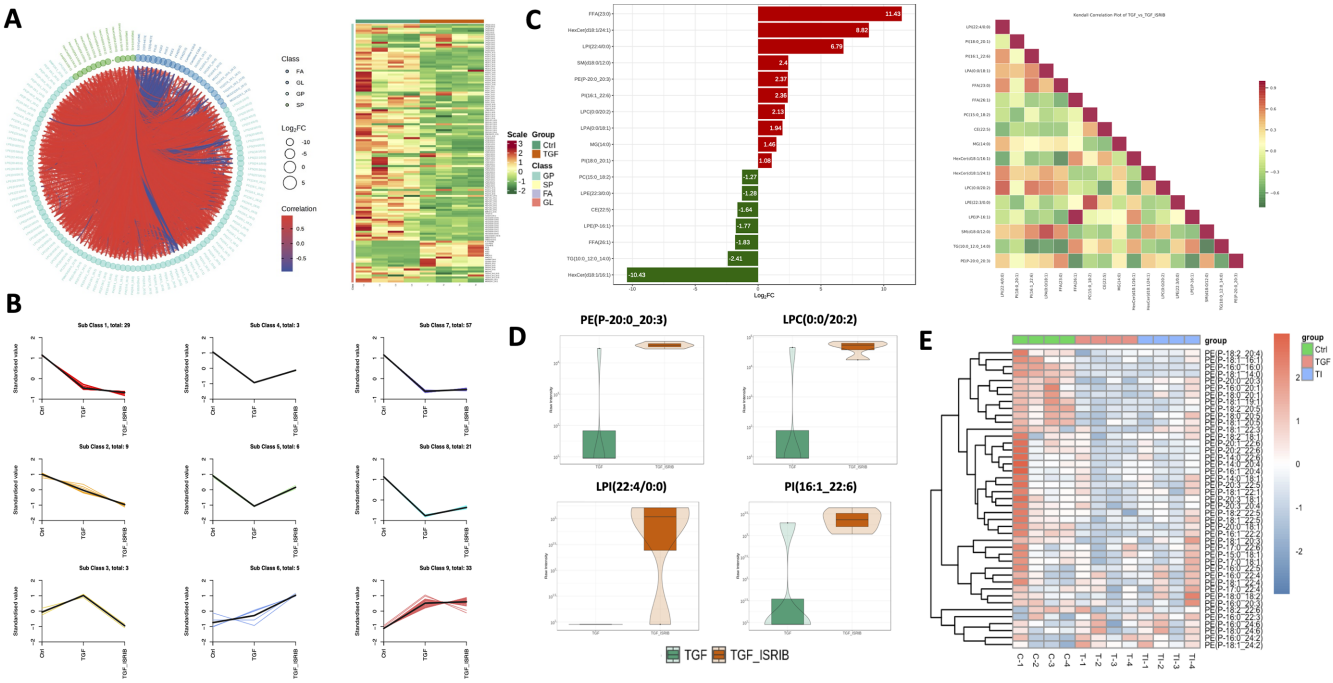

Figure 7. ISRIB regulates phosphatidylethanolamine metabolism in LECs. (**A**) Differential metabolites visualized using a chord diagram and heatmap, depicting the lipid accumulation differences between control and TGFβ2-treated LECs. GL, glycolipids; GP, glycerophospholipids; FA, fatty acid; SP, sphingolipids. (**B**) K-means clustering analysis of lipid species detected in LECs was performed, with the y-axis representing the standardized relative abundance of lipids. (**C**) Top changed metabolites and their correlation matrix between TGFβ2 and the TGFβ2 + ISRIB group. (**D**) Relative content of glycerophospholipids between TGFβ2 and the TGFβ2 + ISRIB group. (**E**) Heatmap of PEs among control (Ctrl), TGFβ2 (TGF), and TGFβ2 + ISRIB (TI) groups.

Investigative Ophthalmology & Visual Science

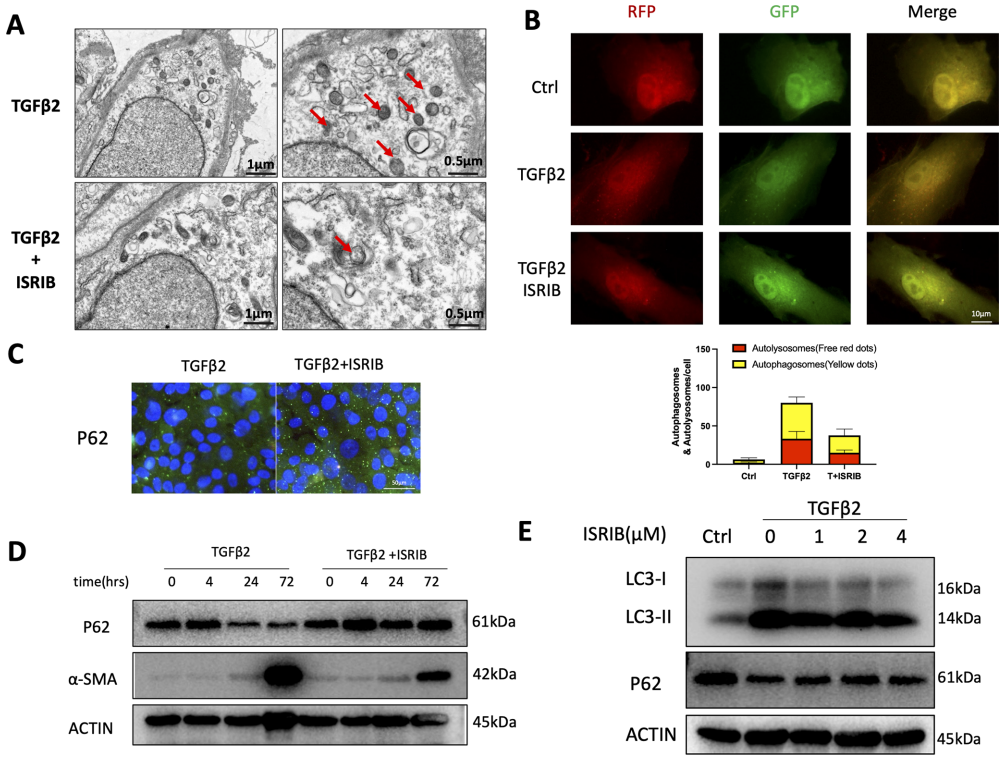

Figure 8. ISRIB attenuates TGFβ2-mediated autophagy. (**A**) Representative transmission electron microscopy (TEM) images of LECs exposed to TGFβ2 and ISRIB for 48 hours. *Red arrows* indicate autophagic vacuoles. (**B**) LECs were infected with the mRFP-GFP-LC3 reporter virus and exposed to TGFβ2 and ISRIB for 48 hours (*red*: autolysosomes; *yellow*: autophagosomes). *Scale bar*: 10 μm. (**C**) Immunofluorescence staining revealed P62 expression in LECs exposed to TGFβ2 and ISRIB for 48 hours. *Scale bar*: 50 μm. (**D**) Western blot analysis of P62 and α-SMA expression levels after cotreatment with TGFβ2 and ISRIB (4 μM) at different time points. (**E**) Western blot analysis of LC3 and P62 expression levels after cotreatment with TGFβ2 and different concentrations of ISRIB.

regulates EMT through autophagy. To this end, we examined the effects of ISRIB on LEC autophagy in the presence of TGFβ2. Transmission electron microscopy revealed abnormally autophagic vacuoles under TGFβ2 stimulation, which were largely abolished by cotreatment with ISRIB (Fig. 8A). Furthermore, we monitored autophagic flux via an mRFP-GFP-LC3 probe in LECs. TGFβ2 incubation resulted in the accumulation of both red and yellow dots, indicating the activation of autophagosome formation and lysosomal degradation (Fig. 8B). However, both red and yellow puncta were markedly reduced in the ISRIB-treated groups compared to those observed during TGFβ2-induced autophagic flux. Immunofluorescence also revealed abundant P62 proteins in ISRIB-treated LECs (Fig. 8C). To further confirm the regulatory role of ISRIB in TGFβ2-mediated autophagy, the levels of autophagy markers were determined by Western blot analysis in time- and dose-dependent manners. Autophagy was activated by 24 hours after TGFβ2 treatment, as manifested by a decrease in the level of the autophagy substrate protein P62. However, ISRIB impaired the turnover of P62 as well as α-SMA production in a time-dependent manner (Fig. 8D). The conversion of MAP1LC3B from its cytosolic form (LC3-I) to its active form (LC3-II) was also evaluated. As shown in Figure 8E, a pronounced increase in LC3 was observed upon TGFβ2 stimulation, whereas ISRIB dose-dependently suppressed LC3-II upregulation.

Autophagy Mediates the Antifibrotic Effects of the ISRIB

To further explore the underlying mechanisms responsible for the antifibrotic function of ISRIB, we conducted immunostaining of BiP and P62 in mouse capsular fibrosis plaques following ISRIB treatment. Compared to the vehicle-treated control group, the ER stress marker BiP was downregulated, while the autophagy marker P62 was upregulated in the fibrotic regions (Fig. 9A). Furthermore, we investigated the effects of the autophagy inducer rapamycin on EMT-related genes in LECs. Interestingly, the ISRIB-mediated suppression of mesenchymal gene expression was diminished by rapamycin (Figs. 9B–D). Moreover, the lysosomal inhibitor chloroquine (CQ) augmented the ability of ISRIB to block α-SMA (Fig. 9D). Taken together, these data indicate that the regulation of autophagic flux by ISRIB is implied in the antifibrotic process.

Discussion

Lens fibrosis, including PCO and ASC, poses a substantial challenge to health care systems and remains one of the major areas of unmet need in clinical ophthalmology. In the present study, we demonstrated sustained activation of ER stress in a mouse model of injury-induced lens fibrosis and also in patients with ASC, which in turn promoted EMT progression. Pharmacologic and genetic inhibition of

Investigative Ophthalmology & Visual Science

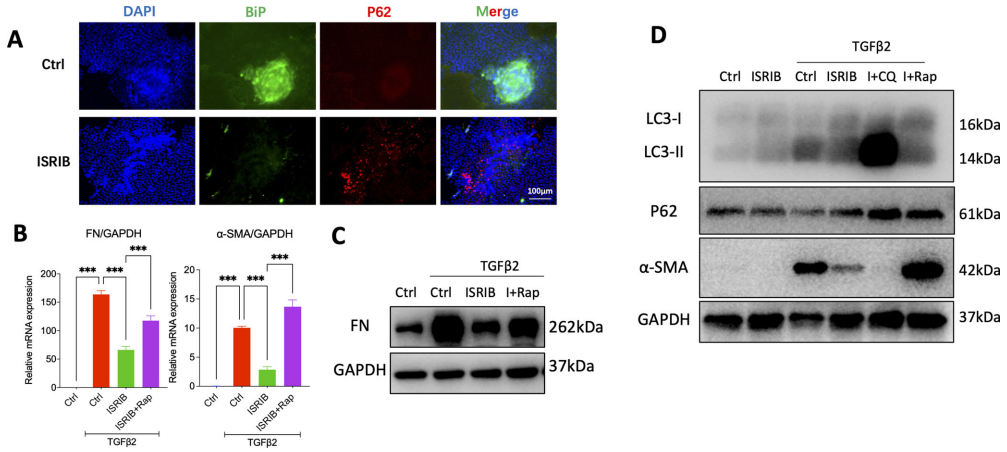

Figure 9. Autophagy mediates the profibrotic effects of ISRIB. (**A**) Immunostaining of BiP and P62 in mouse subcapsular plaques in the control and ISRIB-treated groups. (**B**, **C**) FN and α-SMA expression levels were measured by quantitative RT-PCR and Western blotting in LECs treated with TGFβ2, ISRIB, and rapamycin (250 nM) for 72 hours. (**D**) Western blot analysis of LC3, P62, and α-SMA expression levels in LECs treated with TGFβ2, ISRIB, rapamycin, and CQ (50 μM) for 72 hours.

the PERK/ATF4 branch of the ER stress alleviates TGFβ2-induced EMT, whereas inhibition of the IRE1/XBP1 branch does not alter mesenchymal gene expression. Mechanically, pharmacologic targeting of the PERK/ATF4 pathway with ISRIB suppresses the TGFβ2-mediated autophagy, which is abnormally activated during lens fibrosis. Notably, ISRIB abrogates subcapsular plaque formation through regulating autophagic flux in a mouse model of injury-induced lens fibrosis, providing a promising therapeutic strategy for lens fibrotic diseases.

There is compelling evidence implicating the involvement of ER stress in fibrotic diseases and cancer metastasis, with a focus on the interaction between ER homeostasis and the EMT process. In renal fibrosis, ER stress is activated after unilateral renal ischemia–reperfusion injury, whereas ER stress inhibitors largely block myofibroblast activation.[22] Although many cataractogenic stressors can induce ER stress, including Ca^{2+} imbalance, oxygen imbalance, inflammation, and ischemia,[23] the role of ER stress in lens fibrosis remains unclear. Our previous work demonstrated that ER stress could promote EMT in the human lens epithelial cell line SRA01/04.[24] Duncan and colleagues[25] reported that a low concentration (200 nM) of thapsigargin-coated intraocular lenses inhibited human lens cell growth, but TG induced total death of residual anterior epithelial cells at relatively high concentrations (>2 μM).

During the progression of lens fibrosis, there is an increased need for protein synthesis to support cell hyperproliferation and ECM secretion, leading us to hypothesize that ER stress could be activated when cells cannot meet the high protein-folding demand. In the current study, we observed ER stress marker BiP induction and ER expansion during LECs' EMT, indicating ER stress activation. Moreover, ER stress inducers promoted EMT, whereas the ER stress inhibitor 4-PBA and the PERK inhibitor ISRIB effectively suppressed EMT. Emerging evidence highlights the intricate relationship between ER stress and EMT across various pathological contexts, with the three major ER stress sensors—PERK, IRE1, and ATF6—playing unique regulatory roles.[26] Previous studies show IRE1 also modulates EMT through EMT-TFs such as SNAI1 and ZEB1.[26] However, our data revealed that EMT-related gene expression is selectively correlated with the PERK/ATF4 branch but not with the IRE1 branch. The canonical TGFβ/SMAD2/3 pathway is crucial in EMT and fibrosis. SMAD2/3 phosphorylation, triggered by TGFβ2, forms a Smad complex that translocates to the nucleus to regulate gene transcription.[27] Here, we found that ISRIB could suppress SMAD2/3 activation and nuclear translocation, reducing mesenchymal-related protein expression and counteracting TGFβ2-induced EMT in LECs. Moreover, inhibiting the PERK/ATF4 pathway with ISRIB suppressed SMAD2/3 activation and mesenchymal gene expression, preserving lens transparency after needle injury in mice.

ATF4, a b-ZIP transcription factor of the cyclic-AMP response element-binding family, is a stress-responsive gene regulated by factors such as oxygen deprivation, nutrient deprivation, ER stress, and oxidative stress.[28,29] Under normal conditions, its expression level remains relatively low, but ATF4 is essential for developing multiple organs, including embryonic lens formation, bone development, and fetal liver hematopoiesis, due to its role in transcriptional regulation.[30] More than 25 years ago, ATF4 was first identified as essential for lens development.[31] Tanaka and colleagues[31] reported in 1998 that ATF4 is crucial for the survival of the late embryonic mouse lens, as adult homozygous *Atf4* null mice invariably exhibit severe microphthalmia. Although their primary lens structure remains normal until embryonic day 14.5, the *Atf4* null lens later degenerates due to apoptosis, failing to form secondary fiber cells. This highlights ATF4's essential role in the later stages of lens fiber cell differentiation. However, the underlying molecular mechanisms remain unclear. Later in 2000, Hettmann et al.[32] reported that by embryonic day 14.5, anterior LECs in *Atf4* null mice underwent massive and synchronous apoptosis, leading to the complete resorption of the developing lens, a process mediated by a p53-dependent cell death pathway. Two decades later, Duncan and colleagues[33] further elucidated the role and molecular mechanisms of ATF4 in the latter stages of fetal lens development. Their research not only provides more detailed evidence that ATF4 is required for lens epithelial cell proliferation and survival during late embryonic development but also highlights its essential role in regulating a subset of the

Investigative Ophthalmology & Visual Science

lens-preferred transcriptome, including markers of late fiber cell differentiation such as *DnaseIIb*. Utilizing transcriptomic analysis, they revealed that ATF4 plays a crucial role in nutrient transport and amino acid biosynthesis, which are essential for LEC differentiation in the low-nutrient environment of the lens. Furthermore, unlike ATF4's regulatory role in pathological EMT, *Atf4* null LECs downregulated epithelial markers while upregulating α-SMA expression, which might be associated with impaired differentiation.[33] Expanding on this, our study demonstrates ATF4's function as an ER stress responder in the EMT of LECs and lens fibrosis induced by injury and TGFβ signaling, highlighting its role in maintaining mature lens epithelial homeostasis under pathological fibrotic condition.

Autophagy has been found to be regulated by the PERK/ATF4 pathway in both normal lens development and fibrotic disease.[33,34] The ER stress–mediated unfolded protein response and autophagy are two evolutionarily conserved mechanisms that preserve cellular homeostasis.[35] Converging lines of evidence suggest reciprocal interactions between ER stress and autophagy.[36] The accumulated proteins are targeted for degradation by autophagy to restore ER homeostasis. The PERK/ATF4 axis has been shown to increase autophagy to promote cytoprotective UPR functions in MYC-driven cancers.[37] ATF4 and its downstream factor CHOP are required to increase the transcription of a set of genes implicated in the formation, elongation, and function of the autophagosome, such as Map1lc3B, Atg7, and Sqstm1.[38,39] In contrast, other studies have shown that ER stress inhibits autophagy flux through IRE1 kinase activity.[40] However, the relationship between ER stress and autophagy in the context of lens fibrosis is still not well understood. In our study, we found that TGFβ2 significantly increased the conversion of LC3-I to LC3-II and P62 degradation in LECs, effects that could be blunted by ISRIB. Inducing autophagy with rapamycin significantly rescued mesenchymal gene expression via ISRIB, whereas the autophagy inhibitor CQ produced the opposite effects.

In conclusion, our findings demonstrate the activation of ER stress in lens fibrosis. The PERK branch of the ER stress selectively regulates the EMT process in LECs through autophagy. The PERK inhibitor ISRIB is highly effective at suppressing the development of lens subcapsular plaques and maintaining lens transparency in a mouse model of lens fibrosis. Thus, PERK inhibition may be a potential therapeutic target to reduce EMT and ameliorate fibrotic diseases.

Acknowledgments

Supported by the National Natural Science Foundation of China (Nos. 82201160, 82070944), the Guangdong Basic and Applied Basic Research Foundation (2024A1515013241, 2021A1515111078), the Guangzhou Science and Technology Planning Project (No. 2024A03J0244, 2025A03J3975), and the State Key Laboratory of Ophthalmology, Zhongshan Ophthalmic Center, Sun Yat-Sen University.

Author Contributions: S.H. and X.W. conceived and designed the study. X.W., J.C. and M.H. performed the experiments. B.C. and X.W. performed the analyses. X.W. wrote the paper. S.H. reviewed and edited the manuscript. All authors read and approved the final submitted manuscript.

Availability of Data and Materials: All other data supporting the findings of this study are available from the corresponding authors upon reasonable request.

Disclosure: **X.R. Wang**, None; **B.X. Chen**, None; **J.P. Chen**, None; **M. Huang**, None**; S. Huang**, None

References

1. Apple DJ, Peng Q, Visessook N, et al. Eradication of posterior capsule opacification: documentation of a marked decrease in Nd:YAG laser posterior capsulotomy rates noted in an analysis of 5416 pseudophakic human eyes obtained postmortem. *Ophthalmology*. 2020;127 S29–S42.
2. Taiyab A, Belahlou Y, Wong V, et al. Understanding the role of Yes-associated protein (YAP) signaling in the transformation of lens epithelial cells (EMT) and fibrosis. *Biomolecules*. 2023;13:1767.
3. Vasavada AR, Praveen MR, Tassignon MJ, et al. Posterior capsule management in congenital cataract surgery. *J Cataract Refract Surg*. 2011;37:173–193.
4. Shihan MH, Novo SG, Wang Y, et al. αVβ8 integrin targeting to prevent posterior capsular opacification. *JCI Insight*. 2021;6(21):e145715.
5. Thiery JP, Acloque H, Huang RYJ, Nieto MA. Epithelial-mesenchymal transitions in development and disease. *Cell*. 2009;139:871–890.
6. Wormstone IM, Wormstone YM, Smith AJO, Eldred JA. Posterior capsule opacification: what's in the bag? *Prog Retin Eye Res*. 2021;82:100905.
7. Shihan MH, Kanwar M, Wang Y, Jackson EE, Faranda AP, Duncan MK. Fibronectin has multifunctional roles in posterior capsular opacification (PCO). *Matrix Biol*. 2020;90:79–108.
8. Chen X, Cubillos-Ruiz JR. Endoplasmic reticulum stress signals in the tumour and its microenvironment. *Nat Rev Cancer*. 2021;21:71–88.
9. Heindryckx F, Binet F, Ponticos M, et al. Endoplasmic reticulum stress enhances fibrosis through IRE1α-mediated degradation of miR-150 and XBP-1 splicing. *EMBO Mol Med*. 2016;8:729–744.
10. Ghavami S, Yeganeh B, Zeki AA, et al. Autophagy and the unfolded protein response promote profibrotic effects of TGF-β 1 in human lung fibroblasts. *Am J Physiol Lung Cell Mol Physiol*. 2018;314:L493–L504.
11. Bradley KL, Stokes CA, Marciniak SJ, Parker LC, Condliffe AM. Role of unfolded proteins in lung disease. *Thorax*. 2021;76:92–99.
12. Xiao W, Chen X, Li W, et al. Quantitative analysis of injury-induced anterior subcapsular cataract in the mouse: a model of lens epithelial cells proliferation and epithelial-mesenchymal transition. *Sci Rep*. 2015;5:1–9.
13. Wang X, Wang B, Zhao N, et al. Pharmacological targeting of BET bromodomains inhibits lens fibrosis via downregulation of MYC expression. *Invest Opthalmol Vis Sci*. 2019;60:4748.
14. Chen T, Chen X, Zhang S, et al. The genome sequence archive family: toward explosive data growth and diverse data types. *Genomics Proteomics Bioinformatics*. 2021;19:578–583.
15. CNCB-NGDC Members and Partners. Database Resources of the National Genomics Data Center, China National Center for Bioinformation in 2022. *Nucleic Acids Res*. 2022;50:D27–D38.
16. Novo SG, Faranda AP, Shihan MH, Wang Y, Garg A, Duncan MK. The immediate early response of lens epithelial cells to lens injury. *Cells*. 2022;11:3456.
17. Ma P, Huang J, Chen B, et al. Lanosterol synthase prevents EMT during lens epithelial fibrosis via regulating SREBP1. *Invest Ophthalmol Vis Sci*. 2023;64:12.

18. Ikushima H, Miyazono K. TGFbeta signalling: a complex web in cancer progression. *Nat Rev Cancer*. 2010;10:415–424.
19. Sun Y, Xiong L, Wang X, et al. Autophagy inhibition attenuates TGF-β2-induced epithelial–mesenchymal transition in lens epithelial cells. *Life Sci*. 2021;265:118741.
20. Ferro-Novick S, Reggiori F, Brodsky JL. ER-phagy, ER homeostasis, and ER quality control: implications for disease. *Trends Biochem Sci*. 2021;46:630–639.
21. Shu S, Wang H, Zhu J, et al. Reciprocal regulation between ER stress and autophagy in renal tubular fibrosis and apoptosis. *Cell Death Dis*. 2021;12:1016.
22. Shu S, Zhu J, Liu Z, Tang C, Cai J, Dong Z. Endoplasmic reticulum stress is activated in post-ischemic kidneys to promote chronic kidney disease. *EBioMedicine*. 2018;37:269–280.
23. Ikesugi K, Yamamoto R, Mulhern ML, Shinohara T. Role of the unfolded protein response (UPR) in cataract formation. *Exp Eye Res*. 2006;83:508–516.
24. Zhou S, Yang J, Wang M, Zheng D, Liu Y. Endoplasmic reticulum stress regulates epithelial–mesenchymal transition in human lens epithelial cells. *Mol Med Rep*. 2020;21:173–180.
25. Duncan G, Wormstone IM, Liu CS, Marcantonio JM, Davies PD. Thapsigargin-coated intraocular lenses inhibit human lens cell growth. *Nat Med*. 1997;3:1026–1028.
26. Santamaría PG, Mazón MJ, Eraso P, Portillo F. UPR: an upstream signal to EMT induction in cancer. *J Clin Med*. 2019;8:624.
27. Meng X-M, Nikolic-Paterson DJ, Lan HY. TGF-β: the master regulator of fibrosis. *Nat Rev Nephrol*. 2016;12:325–338.
28. Pakos-Zebrucka K, Koryga I, Mnich K, Ljujic M, Samali A, Gorman AM. The integrated stress response. *EMBO Rep*. 2016;17:1374–1395.
29. Ameri K, Harris AL. Activating transcription factor 4. *Int J Biochem Cell Biol*. 2008;40:14–21.
30. Yang X, Matsuda K, Bialek P, et al. ATF4 is a substrate of RSK2 and an essential regulator of osteoblast biology; implication for Coffin-Lowry syndrome. *Cell*. 2004;117:387–398.
31. Tanaka T, Tsujimura T, Takedsa K, et al. Targeted disruption of ATF4 discloses its essential role in the formation of eye lens fibres. *Genes Cells Devoted Mol Cell Mech*. 1998;3:801–810.
32. Hettmann T, Barton K, Leiden JM. Microphthalmia due to p53-mediated apoptosis of anterior lens epithelial cells in mice lacking the CREB-2 transcription factor. *Dev Biol*. 2000;222:110–123.
33. Xiang J, Pompetti AJ, Faranda AP, et al. ATF4 may be essential for adaption of the ocular lens to its avascular environment. *Cells*. 2023;12:2636.
34. Su S, Shi YT, Chu Y, et al. Sec62 promotes gastric cancer metastasis through mediating UPR-induced autophagy activation. *Cell Mol Life Sci*. 2022;79:133.
35. Dikic I, Elazar Z. Mechanism and medical implications of mammalian autophagy. *Nat Rev Mol Cell Biol*. 2018;19:349–364.
36. Deegan S, Saveljeva S, Gorman AM, Samali A. Stress-induced self-cannibalism: on the regulation of autophagy by endoplasmic reticulum stress. *Cell Mol Life Sci*. 2013;70:2425–2441.
37. Hart LS, Cunningham JT, Datta T, et al. ER stress-mediated autophagy promotes Myc-dependent transformation and tumor growth. *J Clin Invest*. 2012;122:4621–4634.
38. B'Chir W, Maurin AC, Carraro V, et al. The eIF2α/ATF4 pathway is essential for stress-induced autophagy gene expression. *Nucleic Acids Res*. 2013;41:7683–7699.
39. Senft D, Ronai ZA. UPR, autophagy, and mitochondria crosstalk underlies the ER stress response. *Trends Biochem Sci*. 2015;40:141–148.
40. Lee H, Noh JY, Oh Y, et al. IRE1 plays an essential role in ER stress-mediated aggregation of mutant huntingtin via the inhibition of autophagy flux. *Hum Mol Genet*. 2012;21:101–114.